PERFORMANCE OF A HIGH-SPEED CONCATENATED CODED MODULATION SCHEME OVER FADING CHANNELS

Dariush Divsalar and Sam Dolinar
Jet Propulsion Laboratory
California Institute of Technology
{dariush,sam}@shannon.jpl.nasa.gov

ABSTRACT

We design a concatenated code structure with very simple component codes that can be combined with high-order modulations to achieve good power and bandwidth efficiency, and can be iteratively decoded at high data rates using highly parallelized decoders. In this paper we simulate the performance of these codes over additive white Gaussian noise (AWGN) and Rayleigh fading channels.

INTRODUCTION

In this paper we design coding schemes based on serial concatenations of a high-rate Hamming outer code and a simple 2-state rate-1 accumulator inner code. The interleaver between the outer and inner codes has a block structure that allows easy parallelization of the decoding algorithm for applications requiring high-speed decoding. The serially concatenated codes are combined with BPSK, QPSK, 8PSK or 16QAM modulations to give high overall bandwidth efficiencies.

The general structure of a serial concatenation with a "parallel interleaver" is shown in Fig. 1. In this construction of an $(n^O n^I, k^O k^I)$ code, we concatenate k^I outer codes $\{\mathcal{C}_i^O, i = 1, \ldots, k^I\}$ of length and dimension (n^O, k^O) with n^O inner codes $\{\mathcal{C}_j^I, j = 1, \ldots, n^O\}$ of length and dimension (n^I, k^I), via an interleaver π of total size $k^I n^O$. Instead of allowing a completely general interleaver of size $k^I n^O$, we require that π be decomposable into a set of permutations $\{\pi_i^O, i = 1, \ldots, k^I\}$, each of size n^O, applied to the outputs of each of the k^I outer codes separately, followed by a $k^I \times n^O$ rectangular interleaver, followed by a set of permutations $\{\pi_j^I, j = 1, \ldots, n^O\}$, each of size k^I, applied to the inputs of each of the n^O inner codes separately. In the interests of allowing more irregularity, this structure can be generalized to allow the outer codes $\{\mathcal{C}_i^O, i = 1, \ldots, k^I\}$ to have different dimensions $\{k_i^O, i = 1, \ldots, k^I\}$ and the inner codes $\{\mathcal{C}_j^I, j = 1, \ldots, n^O\}$ to have different lengths

This work was performed at the Jet Propulsion Laboratory, California Institute of Technology under contract with the National Aeronautics and Space Administration.

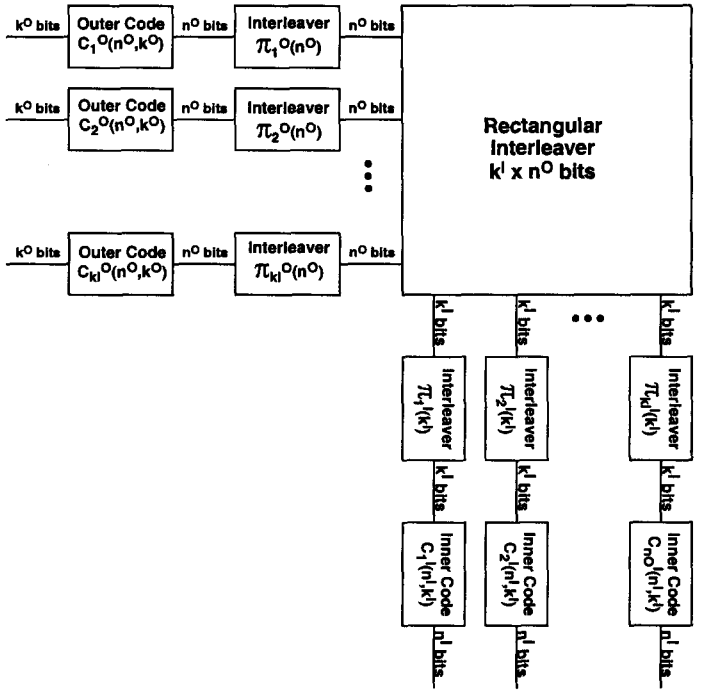

Fig. 1: Serial concatenation with parallel interleaver structure.

$\{n_j^I, j = 1, \ldots, n^O\}$; however, in this paper our attention is restricted to component codes with non-varying dimensions and lengths.

This structure gives a natural generalization of parallel concatenated codes, rather than just an interesting subclass of serially concatenated codes. To see this, simply let all of the k^I outer codes be $(q, 1)$ repetition codes. In this case, the interleavers at the output of the outer codes have no effect and can be omitted. The rectangular interleaver simply ensures that each of the $n^O = q$ inner codes receives a copy of the full package of k^I distinct input bits. Then the random interleavers at the input of the inner codes feed different permutations of these k^I bits to each inner code. The net effect is the same as the usual definition of a parallel concatenated (turbo) code.

When the outer codes are not repetition codes, the interleavers attached to the outer codes can provide some interleaving gain, though this gain will be fairly small if the outer codes are small block codes. For example, an (8,4) extended

Hamming outer code has 14 codewords of weight 4. After a random permutation, these 14 codewords could be scattered into any of $\binom{8}{4} = 70$ weight-4 sequences of length 8. This effectively thins the weight-4 part of the Hamming code's weight spectrum by a factor of 70/14 = 5.

We were interested in the case where the outer component codes $\{\mathcal{C}_i^O, i = 1, \ldots, k^I\}$ are small Hamming codes or extended Hamming codes, and the inner codes are 2-state rate-1 accumulator codes [1]. Our aim was to produce codes with good power and bandwidth efficiencies over a range of bandwidth utilizations, that can be decoded with parallel architecture at very high speeds on the order of 1 Gbps. We wanted outer codes with high code rates for teaming with high-order modulations, and minimum distance 3 or 4 to achieve high interleaving gain. These considerations led to our choice of Hamming or extended Hamming codes as the outer codes that could achieve minimum distance 3 or 4 with the highest code rates for given code dimensions. For the inner codes we selected 2-state rate-1 accumulator codes $1/(1+D)$ for their extreme simplicity of decoding. Since the accumulator codes have the same complexity per bit independent of their length, whereas the decoding complexity of the Hamming codes increases with their lengths, the overall design is asymmetric in the number and sizes of the outer and inner codes, specifically, $n^O \ll k^I$. A goal is select these sizes such that k^I parallel copies of the outer decoder can run at approximately the same speed as n^O parallel copies of the inner decoder.

CODED MODULATIONS USING THE (15,11) HAMMING AND ACCUMULATOR CODES

In this paper we concentrate on one example of the general structure in Fig. 1 in which the outer codes are (15,11) Hamming codes. We team this rate-11/15 code with QPSK, 8PSK, or 16QAM modulation, producing (ideal) bandwidth efficiencies of 1.47 bps/Hz, 2.20 bps/Hz and 2.93 bps/Hz, respectively.

Fig. 2 shows the encoder for a (15,11) Hamming outer code concatenated with a 2-state rate-1 accumulator inner code. For this code, $k^O = 11$, $n^O = 15$, and we selected $k^I = n^I = 372$ to yield an overall code of length 5580 and dimension 4092. In our implementation we used $n^O = 15$ random interleavers $\{\pi_i^O, i = 1, \ldots, n^O\}$ at the output of the Hamming outer codes and $k^I = 372$ S-random [2] interleavers $\{\pi_j^I, j = 1, \ldots, k^I\}$ to permute the inputs to the accumulator inner codes. In the figure we indicate that a desired input data rate of 1.116 Gbps can be obtained by running the 372 Hamming encoders at 3 Mbps each, and the 15 accumulator encoders at 101 Mbps each.

The outputs of the 15 accumulator codes are mapped to a high-order modulation. With 8PSK the first output bits of

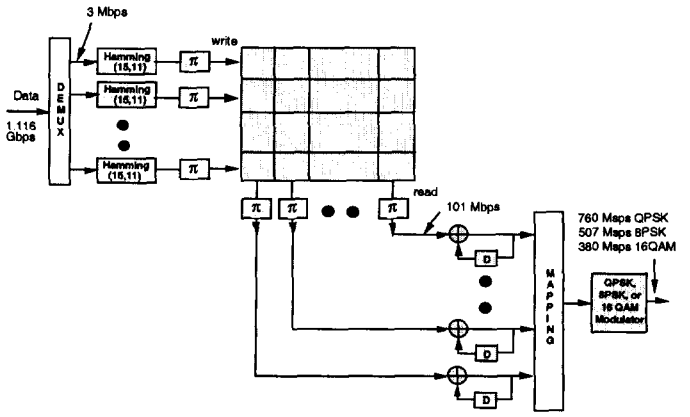

Fig. 2: Encoder for the Hamming and accumulator code.

the first three accumulators are mapped to a 3-bit 8PSK symbol using a Gray code mapping. Then the first output bits of the next three accumulators are mapped to the second 3-bit 8PSK symbol and so on, until the first five 8PSK symbols are produced. Then the next five 8PSK symbols are created using the second bits from three accumulators at a time, and so forth. With QPSK or 16QAM we take output bits two or four at a time from two or four separate accumulators to form each QPSK or 16QAM symbol, stepping through the 15 accumulator codes in a cyclic order until all 5580 output bits are mapped. This type of mapping eliminates the need for a channel interleaver within the length of a code block.

Fig. 3 shows the decoder for the code in Fig 2. In

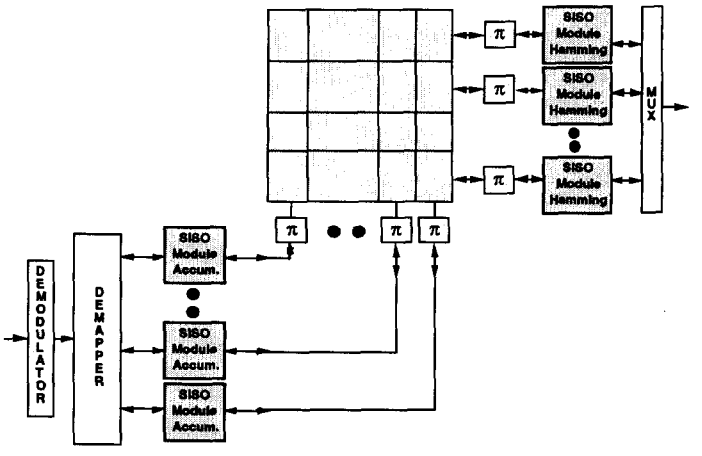

Fig. 3: Decoder for the Hamming and accumulator code.

this figure the demapper provides the reliability of those bits assigned to the modulation symbols, given inphase and quadrature received observations. The Soft-In Soft-Out (SISO) modules for the accumulator can also interact with the demapper for further performance enhancement if desired.

An (n, k) Hamming code has a cyclic representation, and can be equivalently generated as a recursive terminated con-

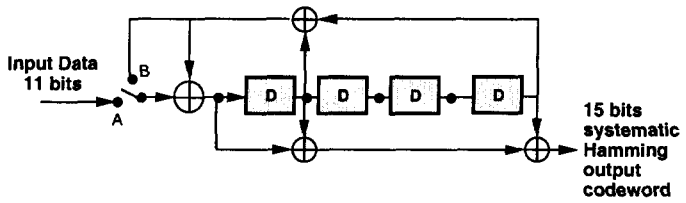

Fig. 4: A recursive convolutional code with primitive feedback polynomial that generates a time-invariant trellis representation that can be used for decoding the (15,11) Hamming code.

volutional code with primitive feedback polynomial. If the feedforward polynomial is chosen to be the same as the feedback polynomial, this produces a systematic version of the Hamming code. This convolutional encoding of the (15,11) Hamming code is shown in Fig. 4. The first k bits enter the systematic convolutional encoder and emerge as the first k encoded symbols. After k bits, the switch in Fig. 4 is toggled and the encoder continues running long enough to produce $n-k$ additional encoded symbols, which are the parity symbols for the (n, k) Hamming code. We note that an extended Hamming code, shortened by one bit, can also be implemented by a recursive convolutional code, where the primitive feedback and feedforward polynomials should be multiplied by $1 + D$.

The convolutional encoding of an (n, k) Hamming code gives a time-invariant trellis representation with 2^{n-k} states. Alternatively, a time-varying minimal trellis representation can be used for decoding to gain speed if necessary over that provided by the time-invariant trellis representation. Fig. 5 shows a minimal trellis representation for the (15,11) Hamming code. The time-invariant trellis corresponding to the

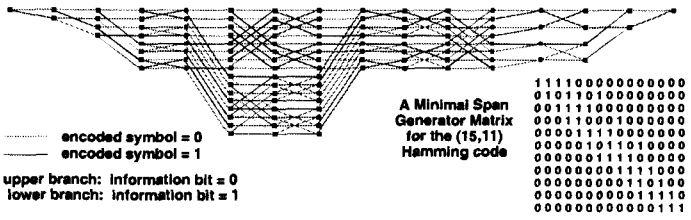

Fig. 5: A time-varying minimal trellis representation that can be used for decoding the (15,11) Hamming code.

convolutional encoder of Fig. 4 has 32 edges per decoded bit, whereas the time-varying trellis of Fig. 5 has only 17.8 trellis edges (on the average) per decoded bit, a reduction of nearly a factor of 2.

The inner accumulator code can be decoded using the BCJR algorithm [3] on a time-invariant trellis with only two states. Alternatively, the accumulator code can also be decoded using belief propagation on a loop-free, highly parallelizable Tanner graph [4] representing the same code, as shown in Fig. 6.

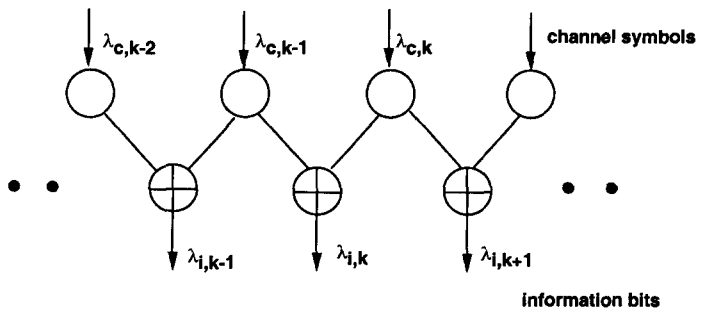

Fig. 6: A Tanner graph representation of the accumulator code that can be used for high-speed parallelizable decoding.

If higher speeds and many iterations are necessary, the inner or outer decoders can pipeline their iterations as needed.

PERFORMANCE ON AN AWGN CHANNEL

First we applied Gaussian density evolution [5, 6] to analyze the performance of concatenated Hamming and accumulator codes under iterative decoding on an additive white Gaussian noise (AWGN) channel. The results are shown in Fig. 7, which plots the output signal-to-noise ratio $\mathrm{SNR_{out}}$ versus the input signal-to-noise ratio $\mathrm{SNR_{in}}$ of the extrinsic log-likelihood messages computed by the outer and inner component decoders. The iterative decoding thresh-

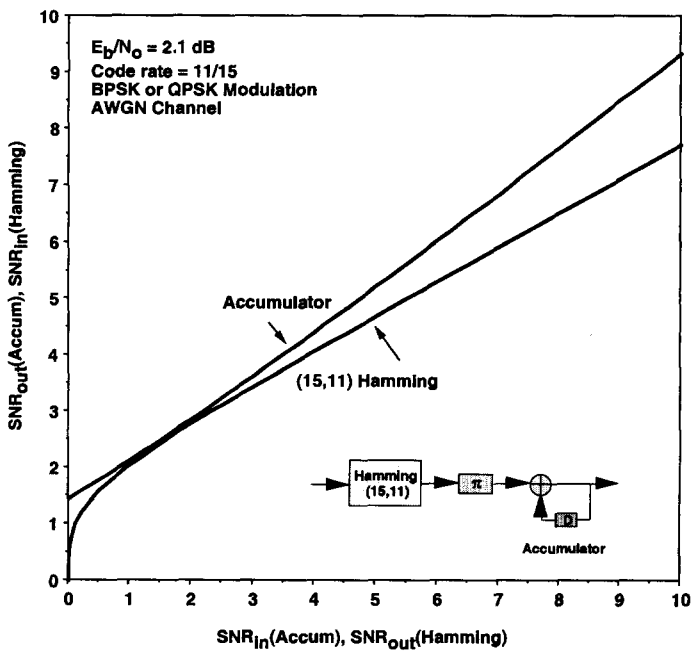

Fig. 7: Gaussian density evolution for the Hamming and accumulator code on the AWGN channel.

old for this code on the binary-input AWGN channel is $E_b/N_0 = 2.1$ dB, which is only 0.6 dB worse than the capacity threshold of 1.5 dB for any code of rate 11/15.

Next we simulated the performance of the (5580, 4092) Hamming and accumulator code when combined with vari-

ous modulations. Figs. 8, 9 and 10 show the performance of this code with QPSK, 8PSK and 16QAM, respectively, on the AWGN channel.

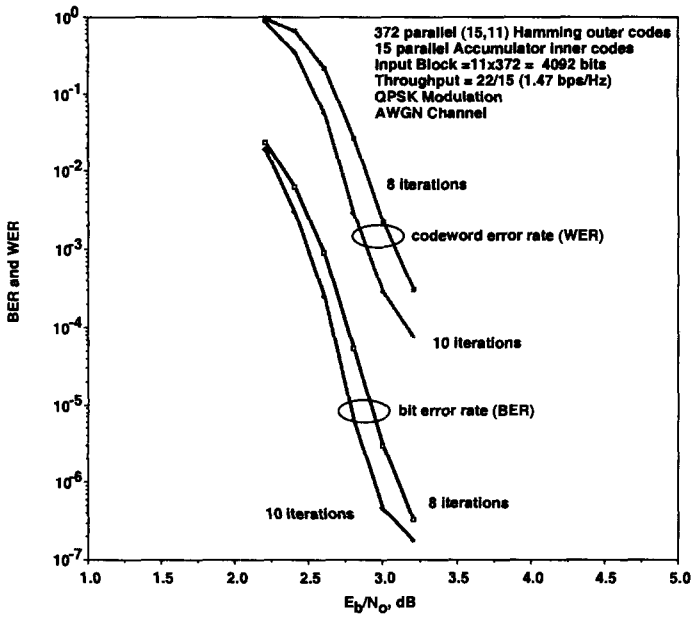

Fig. 8: Performance of the (15,11) Hamming code concatenated via a parallelized interleaver with the 2-state accumulator code, when combined with QPSK modulation on an AWGN channel.

PERFORMANCE ON A RAYLEIGH FADING CHANNEL

We applied Gaussian density evolution [5, 6] to analyze the performance of concatenated Hamming and accumulator codes under iterative decoding on an independent Rayleigh fading channel with perfect channel state information. The results are shown in Fig. 11. The iterative decoding threshold for this code and channel is $E_b/N_0 = 3.8$ dB.

We simulated the performance of the (5580, 4092) Hamming and accumulator code when combined with 8PSK and 16QAM modulations on a correlated Rayleigh fading channel, where the ratio of the maximum Doppler rate f_d to the modulation transmission rate R_s is set as a parameter. The fading process was generated by passing a complex white Gaussian process through a filter with transform function $H(f) = \sqrt{S(f)}$, where $S(f)$ is the power spectral density of the fading process and is modeled for an omnidirectional antenna as $S(f) = C/\sqrt{1-(f/f_d)^2}$, where C is a constant.

Figs. 12 and 13 show the bit error rate (BER) and codeword error rate (WER) with 8PSK and 16QAM, respectively, and no channel interleaving, for $f_d/R_s = 0.05$. For slower fading, with f_d/R_s significantly less than 0.05, channel interleaving over multiple codewords is required to obtain good performance.

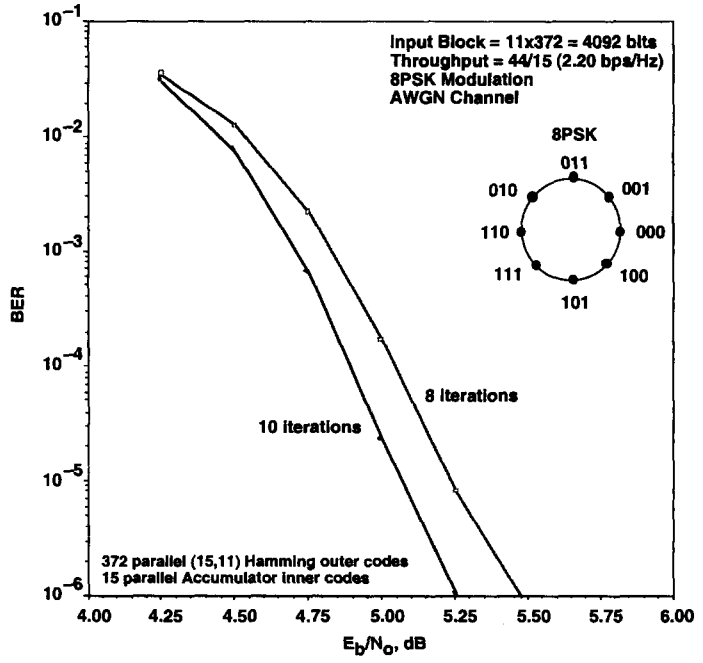

Fig. 9: Performance of the (15,11) Hamming code concatenated via a parallelized interleaver with the 2-state accumulator code, when combined with 8PSK modulation on an AWGN channel.

CONCLUSION

The concatenated codes described in this paper achieve medium-to-high code rates using very simple component codes, and can be combined with high-order modulations to obtain good power and bandwidth efficiency at very high decoding rates.

REFERENCES

[1] D. Divsalar, H. Jin, and R. J. McEliece, "Coding Theorems for 'Turbo-Like' Codes," 1998 Allerton Conference, September 23-25, 1998.

[2] S. Dolinar and D. Divsalar, "Weight Distributions for Turbo Codes Using Random and Nonrandom Permutations," *The Telecommunications and Data Acquisition Progress Report 42-122, April–June 1995*, Jet Propulsion Laboratory, Pasadena, California, pp. 56–65, August 15, 1995.

[3] L. R. Bahl, J. Cocke, F. Jelinek, and J. Raviv, "Optimal Decoding of Linear Codes for Minimizing Symbol Error Rate," *IEEE Trans. Inform. Theory*, vol. IT-20, pp. 284–287, 1974.

[4] R. M. Tanner, "A recursive approach to low complexity codes", IEEE Trans. Information Theory, pp. 533-547, 1981.

[5] H. El Gamal and A. R. Hammons, Jr., "Analyzing the turbo decoder using the Gaussian approximation", ISIT 2000, p. 319. Also submitted to IEEE Trans. Inform. Theory, January, 2000.

[6] D. Divsalar, S. Dolinar, and F. Pollara, "Iterative Turbo Decoder Analysis Based on Density Evolution," *IEEE Journal on Selected Areas in Communications*, Vol. 19, No. 5, pp 891-907, May 2001.

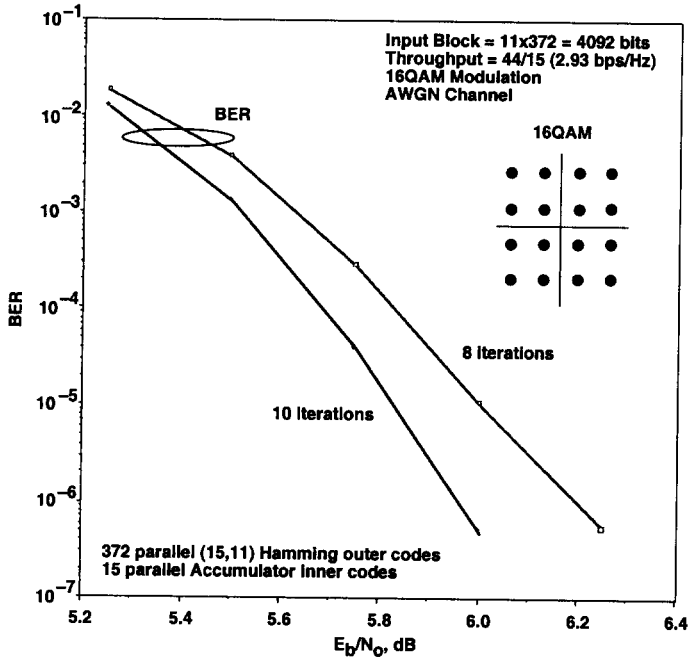

Fig. 10: Performance of the (15,11) Hamming code concatenated via a parallelized interleaver with the 2-state accumulator code, when combined with 16QAM modulation on an AWGN channel.

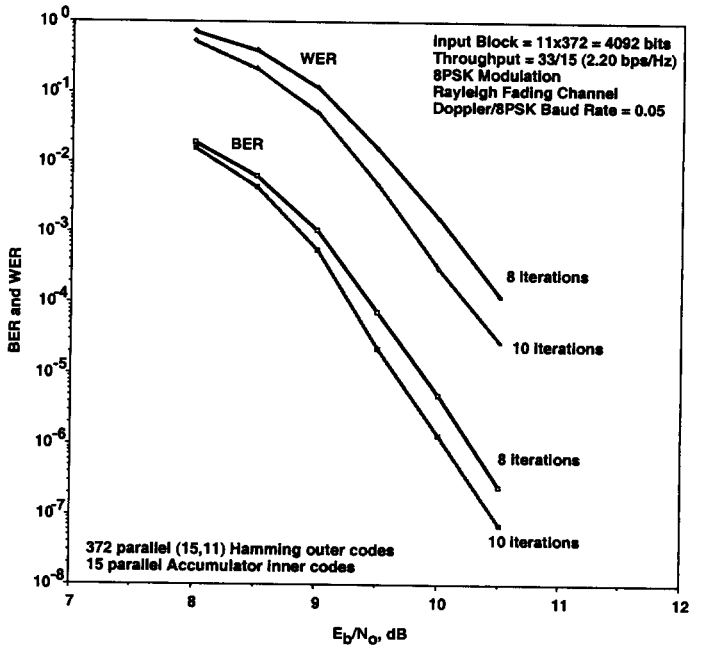

Fig. 12: Performance of the (15,11) Hamming code concatenated via a parallelized interleaver with the 2-state accumulator code, when combined with 8PSK modulation on a correlated Rayleigh fading channel.

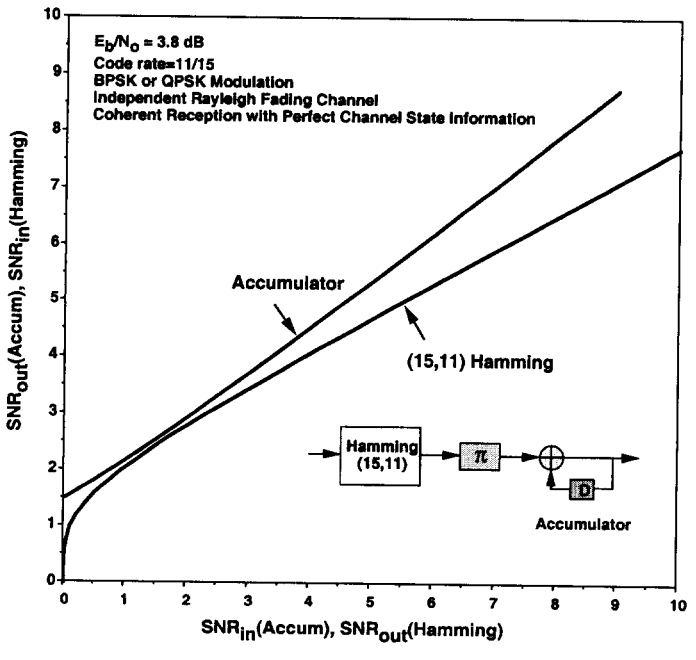

Fig. 11: Gaussian density evolution for the Hamming and accumulator code on an independent Rayleigh fading channel.

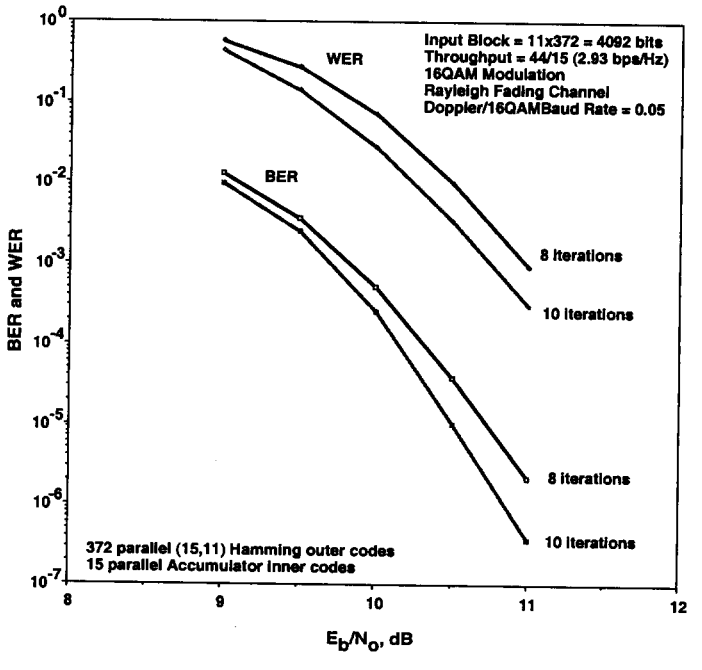

Fig. 13: Performance of the (15,11) Hamming code concatenated via a parallelized interleaver with the 2-state accumulator code, when combined with 16QAM modulation on a correlated Rayleigh fading channel.